AD_____

Award Number: W91XWH-06-1-0113

TITLE: Parallel Genomic and Chemical Screens to Identify Both Therapeutic Targets and Inhibitors of These Targets in the Treatment of Neurofibromatosis

PRINCIPAL INVESTIGATOR: Norbert Perrimon Ph.D.

CONTRACTING ORGANIZATION: Harvard Medical School
                           Boston, MA 02115

REPORT DATE: December 2006

TYPE OF REPORT: Final

PREPARED FOR: U.S. Army Medical Research and Materiel Command
               Fort Detrick, Maryland 21702-5012

DISTRIBUTION STATEMENT: Approved for Public Release;
                        Distribution Unlimited

REPORT DOCUMENTATION PAGE

1. REPORT DATE	2. REPORT TYPE	3. DATES COVERED
01-12-2006	Final	15 Nov 2005 – 14 Nov 2006

4. TITLE AND SUBTITLE

Parallel Genomic and Chemical Screens to Identify Both Therapeutic Targets and Inhibitors of These Targets in the Treatment of Neurofibromatosis

5a. CONTRACT NUMBER

5b. GRANT NUMBER
W81XWH-06-1-0113

5c. PROGRAM ELEMENT NUMBER

6. AUTHOR(S)

Norbert Perrimon Ph.D.

Email: perrimon@receptor.med.harvard.edu

5d. PROJECT NUMBER

5e. TASK NUMBER

5f. WORK UNIT NUMBER

7. PERFORMING ORGANIZATION NAME(S) AND ADDRESS(ES)

Harvard Medical School
Boston, MA 02115

8. PERFORMING ORGANIZATION REPORT NUMBER

9. SPONSORING / MONITORING AGENCY NAME(S) AND ADDRESS(ES)
U.S. Army Medical Research and Materiel Command
Fort Detrick, Maryland 21702-5012

10. SPONSOR/MONITOR'S ACRONYM(S)

11. SPONSOR/MONITOR'S REPORT NUMBER(S)

12. DISTRIBUTION / AVAILABILITY STATEMENT
Approved for Public Release; Distribution Unlimited

13. SUPPLEMENTARY NOTES
Original contains colored plates: ALL DTIC reproductions will be in black and white.

14. ABSTRACT

In model systems, such as Drosophila, high-throughput genetic and chemical screens are powerful tools to elucidate the components and inhibitors of signaling pathways. The success of these screens is dependent on the development of experimental assays which serve as readouts of pathway activity. However, to date no such assay has been developed to monitor the activity of Nf1 or Nf2. Here we describe the development a novel technology that can be used to rigorously quantify and analyze single-cell morphology in an automated fashion. As a proof-of concept we have analyzed morphological data derived from 249 different conditions, and defined phenoclusters of functionally related genes. We observe that Nf1 and Nf2 are members of distinct phenoclusters, and that other genes in these clusters may be highly relevant to understanding role of Nf1 and Nf2 in promoting disease. With the successful development of methods to determine quantitative phenotypic profiles of cells, performing screens for genetic or chemical modifiers of Nf1 or Nf2 is now feasible.

15. SUBJECT TERMS
Phenotypic Profiling, High-throughput screening, Genetic Modifiers, Morphology

16. SECURITY CLASSIFICATION OF:			17. LIMITATION OF ABSTRACT	18. NUMBER OF PAGES	19a. NAME OF RESPONSIBLE PERSON USAMRMC
a. REPORT	**b. ABSTRACT**	**c. THIS PAGE**	UU	23	**19b. TELEPHONE NUMBER** *(include area code)*
U	U	U			

Table of Contents

Parallel Genomic and Chemical Screens to Identify both Therapeutic Targets, and Inhibitors of these Targets, in the Treatment of Neurofibromatosis.

Introduction

Neurofibromatosis type I (NF1) results following mutations in the *Nf1* gene which encodes a Ras GTPase activating protein (RasGAP), whereas the rarer disorder Neurofibromatosis type II results following loss of function mutations in the *Nf2/merlin* gene. In healthy organisms, Nf1 regulates cell growth and proliferation through the modulation of Ras (*1*), and loss of Nf1 leads to tumor formation due to the subsequent hyperactivation of Ras (*2*). Nf2/merlin promotes the establishment of cell polarity, cell-cell junctions, and of adherence structures that link the cell to the extracellular matrix (ECM). Mutations in *Nf2/merlin* contribute to the progression of NF2 disease by desensitizing the proliferation and migratory machineries to the inhibitory signals that emanate from neighboring cells and the ECM (*3*). However to date there is not a complete understanding as to identity or function of the specific signaling proteins that act upstream or downstream of Nf1 and Nf2.

Using high-throughput cell-based RNAi screens, our laboratory has systematically elucidated the majority, if not all, of the components involved in canonical signaling pathways such as the Wnt, Hedgehog (Hh), MAPK, and JAK-STAT pathways (*4-7*). Each particular screen made use of unique experimental readouts of pathway activity. For example, in the case of Wnt, Hh, or JAK-STAT screens , we monitored transcription of luciferase reporter genes placed downstream of pathway-specific promoters (*4-6*). Alternatively, to identify MAPK components, we monitored phosphorylation of ERK protein (*7*). We reasoned that although genome-wide RNAi screens could also be used to identify components of Nf1 and Nf2/merlin regulated signaling pathways, we first had to develop an experimental readout of Nf1 and/or Nf2 activity.

4

Body

Aim 1: Describe the phenotype of Drosophila S2R+ and cells and Kc cells which have been treated with dsRNA targeting Drosophila Nf1 and Nf2 genes.

Aim 1a) Determine if inhibition of Nf1 and/or Nf2 leads to changes in the phosphorylation state of MAPK as compared to untreated cells.

Given the well-established role of Nf1 in regulating Ras signaling, and the increase in MAPK/ERK phosphorylation observed in Nf1-deficient flies (*8*), we expected to observe increased phosphorylation of MAPK/ERK following inhibition of Nf1. Furthermore, increases in MAPK signaling are also a characteristic of Nf2-deficient tumor cell lines (*9*). However we did not observe that RNAi of either *Drosophila Nf1* or *Nf2* significantly increased or decreased the levels of phosphorylated *Drosophila* MAPK/ERK in S2R+ or Kc cells lines in either starved or stimulated conditions (*7*).

b) Determine if inhibition of Nf1 and/or Nf2 leads alterations in cellular morphology.

As dysregulation of Nf1 and Nf2 signaling leads to tumorigenesis which typically involves alterations in cell and tissue morphology, we used conventional fluorescence microscopy to analyze the phenotype of GFP-transfected *Drosophila* cells where *Nf1* or *Nf2/merlin* genes are silenced by dsRNA. However, unlike the MAPK/ERK studies performed in Aim 1a, we inhibited *Nf1* or *Nf2* by RNAi in Drosophila BG-2 cells. Control/wild-type BG-2 cells are a highly motile cell line that resemble mammalian fibroblast cells in that during migration cells exhibit a polarized leading edge with extensive lamellipodial protrusions (Figure 1A). In addition, BG-2 cells coordinate the formation of lamellipodia with retraction of the cell body at the rear of the moving cell (Figure 1A). We observed that silencing of *Nf1* and *Nf2* by dsRNA dramatically affects the cellular morphology of *Drosophila* BG-2 cells in similar, yet distinct fashions (Figure 1B and 1C). RNAi of *Nf1* results in unpolarized cells with defects in lamellipodia formation that also appear retracted compared to wild-type cells (Figure 1B). The phenotype of BG-2 cells where *Nf1* is silenced is remarkably consistent with previous studies of mammalian

astrocytes which reported defects in cell spreading, migration, and attachment following a loss of a single copy of *Nf1* (*10*). Targeting *Nf2* for dsRNA-mediated silencing also results in highly-rounded and retracted cells with no lamellipodial protrusions and loss of polarity (Figure 1C). However cells where Nf2 is inhibited appear to have no protrusions whatsoever, whereas cell treated with *Nf1* dsRNA still have a number of filamentous processes (Figure 1B, chevrons). We speculate that silencing *Nf2/merlin* by dsRNA results in round cells with no clear leading edge due to the fact that these cells are unable to form proper adhesions to the ECM, a model consistent with the role of Nf2 in regulating the formation of adhesive structures (*3*). Taken together, this data suggests that Nf1 and Nf2 function normally to regulate pathways that regulate cellular morphology.

c) Changes in proliferation.

As well-characterized tumor suppressors we speculated that using dsRNA-mediated gene silencing of *Nf1* or *Nf2* may lead to increased cell proliferation. However, using an assay previously developed in our laboratory to accurately determine cell viability and proliferation following the treatment of cells with dsRNA targeting genes of interest (*11*), we did not observe that inhibition of *Nf1* or *Nf2* in Kc, S2R+, or BG-2 cells leads to significant increases, or decreases, in proliferation (Data not shown). One potential explanation for our failure to detect increased levels of proliferation following dsRNA-mediated silencing of *Nf1* or *Nf2* is that transient inhibition of these genes in tissue culture cells is not sufficient to induce similar increases in proliferation as observed when these genes are deleted in NF patients or model organisms (*3, 12*).

Aim 2: Perform genome-wide screen for dsRNAs which result in reversion of the phenotypes observed following RNAi of Nf1 or Nf2.

We observed that inhibiting Nf1 and Nf2 by dsRNA dramatically affected the cellular morphology of *Drosophila* BG-2 cells in highly diverse fashions (Figure 1). As such we reasoned that we could perform large-scale genetic screens for genes that suppressed, enhanced, or altered the morphological phenotype of cells where Nf1 or Nf2 activity is inhibited, and we could begin to determine components of Nf1 and Nf2 regulated signaling networks.

The analysis of cellular phenotypes following the systematic inhibition of genes has been extensively used in *C. elegans* not only to determine genes involved in the regulation of morphology, but to model networks of functionally related genes (*13, 14*). Furthermore, our own lab has performed large-scale studies to identify *Drosophila* genes involved in the regulation of cell shape (*15*). However, all these studies performed to date have been <u>qualitative</u> in nature as individual cellular phenotypes and morphologies were observed, and interpreted by, human experimentalists. We reasoned that in order to perform systematic screens for genes involved mediating the effects on morphology resulting from RNAi of *Nf1* and *Nf2*, that such screens must be <u>quantitative</u> in nature. Furthermore, because previous screens have involved manually curating thousands of images, which requires a large amount of time, we aimed to automate the execution of our experiments and analysis as much as possible. **Thus prior to beginning a screen for genetic modifiers of *Nf1* or *Nf2*, we aimed to develop a novel method in order to quantify single-cell morphology in an automated fashion.**

The major challenge in quantifying morphology is accurately defining cellular boundaries, in an automated fashion, in image fields which might contain dozens, if not hundreds of individual cells. Once the cell borders have been defined, and "cell segments" created, quantification of the segments is

relatively trivial. Therefore in order to obtain accurate segmentation of single-cells, we image and segment single-cells that are stochastically labeled with GFP. Stochastic labeling is accomplished by transient transfection of BG-2 cells with plasmids encoding GFP, which is relatively inefficient (~15-20% of cells become transfected). Although obtaining feature values from GFP-labeled cells versus the entire cell population in the image greatly reduces the number of cells analyzed in each treatment, stochastic labeling ensures accurate and precise cell segmentation that would otherwise be impossible. Our segmentation algorithm uses intensity thresholds to identify cells, and is based on the assumption that sharp decreases in intensity levels represent cellular boundaries. We further refined the segmentation used for the analysis by creating CellSegmenter, a GUI whereby a user can manually adjust intensity thresholds until they accurately match the boundaries of the cell, separate two or more distinct cells which have been erroneously defined as a single cell by the algorithm, and select cell segments that are considered good representations of cellular boundaries (Figure 2A). Thus, while the segmentation procedure is not fully automated, we feel that this method ensures a data set of very high quality. We quantified approximately 150 different features for individual cells that reflected basic aspects of cell geometry, detailed aspects of cellular protrusions, or the distribution of GFP intensity within the cellular boundaries (Figure 2B). Following segmentation and quantification, single cell data is used to calculate mean feature values for the condition of interest. Each vector of 150 different features is termed a "phenotypic signature".

In order to test our methods, we generated a dataset comprised of 249 different conditions corresponding to: (1) The overexpression by transient transfection of 20 different RFP-tagged mutant forms of Rho GTPases, RhoGEFs, kinases, and other regulators of the microtubule and actin cytoskeletons. (2) 173 dsRNAs chosen at random from a larger collection of dsRNAs targeting all known GTPases, GEF, GAPs, and other genes implicated in cytoskeletal organization. Notably, this collection of dsRNA overlaps considerably with the collection of ~900 dsRNAs used by our lab in previous

8

morphological screens (*15*). (3) An additional 45 dsRNAs targeting the majority of known *Drosophila* RhoGEFs, GAPs, and GTPases (4) Overexpression of an activated form of the RhoGEF Sif/still-life in combination with various dsRNAs chosen at random.

Although a phenotypic signature is composed of ~150 different features, we hypothesized that only a subset of these features would be informative and useful in further classification of genes and conditions. In fact, hierarchical clustering of all conditions by all features does not reveal that genes/conditions cluster in meaningful or interpretable fashions (Data not shown). Presumably this is due to the fact that the values for many features correlated with each other, and that all features values are not relevant to distinguishing different aspects of morphology. Thus, we aimed to reduce the dimensionality of the data by using Neural Network based methods to generate classifiers that represent a non-linear function in a multi-dimensional space that segregates the majority of cells from a condition of interest (i.e. RacV12 overexpressing cells), from other conditions. Seventeen distinct conditions were chosen for analysis based on the fact that their phenotypes were qualitatively distinctive and discernable from control cells (Table 1). For example overexpression of an N-terminally truncated form of the RhoGEF still-life/Sif (ΔN-Sif), the *Drosophila* orthologs of mammalian Tiam-1, stimulates extensive lamellipodia formation, cell spreading, and a general loss of tension demonstrated by the flat and thin appearance of the ΔN-Sif cells. Importantly, we did not attempt to generate classifiers for phenotypes that were not qualitatively distinctive from control cells regardless of the construct or dsRNA used (i.e. Cdc42 dsRNA treated cells appeared largely similar to control cells). Conversely, we derived classifiers for particular states and phenotypes even if little is understood as to the underlying mechanisms that led to the particular phenotype. For example, ΔN-RhoGEF3 and CG3799 overexpression each promotes distinctive changes in cell morphology, but the specificity of these RhoGEFs for particular GTPase targets is unknown.

9

In order to extract functional grouping of genes from our dataset each cell state is scored using 7/9 successfully derived classifiers, and subsequently clustered using hierarchical methods. The 7-component vector assigned to each cell state is comprised of Z-scores representing how phenotypically similar the population of cells of that state are to cells of the state from which each classifier was generated compared to an equally sized population of cells chosen at random. We term this Z-score a "certainty of classification score". For example, for cells where CG10188 (a RhoGEF) has been targeted by dsRNA the certainty of classification score for the RacF28L classifier is 0.335288, which indicates that CG10188 dsRNA induces a morphology that is slightly more "RacF28L-like" than an equal number of randomly chosen cells. By contrast, the Z-score for RacF28L cells on the RacF28L classifier is 18.222. The 7 Z-scores that make up the vectors are certainty of classification scores for the RacV12, RhoF28L, RhoV14, RhoF30L, CG3799 full-length, ΔN-Sif, and ΔN-RhoGEF3 classifiers. Although the classifiers trained against the combination of RhoV14-RhoF30L and RacV12-RacF28L expressing cells both have acceptable levels of sensitivity and specificity, we choose not to include these scores in our clustering due to the fact that RhoV14/RhoF30L cells are highly morphological diverse (thus a high score on this classifier is largely not interpretable), and that RacV12/RacF28L are highly phenotypically similar (thus do not provide information beyond the individual classifiers themselves).

Two-dimensional hierarchical clustering of cell states by the 7 component vector reveals that genes fall into several distinct clusters. As expected, genes will similar phenotypes cluster tightly together, which strongly validates the methodologies used in this study and highlights the fact that we have successfully developed a technique to quantitatively determine and classify cell morphology (Figure 3). We define "phenoclusters" as genes grouped by having a correlation score of greater than 0.80 (Figure 3). A correlation of 0.80 was determined based on the fact that clusters defined by correlation scores less that 0.80 group phenotypically diverse cells, whereas determining clusters of genes by scores greater that 0.80 results in phenotypically similar cells falling into separate clusters.

We speculate that the genes that are members of particular phenoclusters may act in linear or parallel fashion to regulate a common biological function, similar to genetically interacting genes. RNAi of *Nf2/merlin* results in a phenotype that clusters with phenotypes resulting from RNAi of a number of known components of Rho signaling pathways such *Rho-like*, *p190RhoGAP*, *SCAR* and *RhoGEF3* (Figure 3B). The finding that the morphology of cells where *Nf1* has been silenced is quantitatively similar to the morphology following the inhibition of a number of components of Rho GTPase signaling pathways is remarkably consistent with previous observations that Nf2 regulates, and is regulated by Rho signaling (*3*). Furthermore, *Nf2* RNAi clusters with RNAi of a number of genes known to regulate adherence structures such as *Gef26* (*16, 17*)*, Arm* (*18*)*,* and *Ankyrin* (*19*)which supports a model that Nf2 is involved in the regulation of adherence and inhibition of Nf2 signaling results in a failure of cells to attach to the ECM, and consequently induce protrusive activity (Figure 3B). **Importantly, these genes are excellent candidates for genes involved in the progression of Neurofibromatosis Type II, and might represent therapeutic targets for treatment of the disease.**

Nf1 RNAi is a member of a related, but quantitatively distinct phenocluster that contains only the genes *CG1193, CG6017, Rab3,* and *yurt* (Figure 3C). Although the genes are mostly uncharacterized, we propose they are also likely involved in regulating similar biological processes as *Nf1*. Akin to genes that cluster with *Nf2*, we hypothesize these genes are potentially involved in the progression of Neurofibromatosis Type I disease. Intriguingly, the mammalian homologs of *Drosophila* Yurt are FERM domain-containing proteins and are highly related to mammalian Nf2/merlin (*20, 21*), and yurt may represent a point of cross-talk between Nf1 and Nf2 signaling pathways.

In conclusion, we have developed a novel technology that can be use to rigorously quantify and analyze single-cell morphology in an automated fashion. As a proof-of-concept we have analyzed morphological data derived from 249 different conditions, and defined phenoclusters of functionally related genes. We observe that *Nf1* and *Nf2* are members of distinct phenoclusters and that other genes in these clusters may be highly relevant to understanding role of *Nf1* and *Nf2* in promoting disease. **Furthermore, with the successful development of methods to determine quantitative phenotypic profiles of cells, performing screen for genetic or chemical, modifiers of *Nf1* or *Nf2* is now feasible.**

Key Research Accomplishments

- We have developed a novel system to rigorously quantify and analyze single-cell morphology in an automated fashion. This novel technology can be combined with RNAi-based genetic screening methods to systematically query the role of genes in the regulation of cell shape, and describe functionally related genes.

- We have identified genes functionally related to both Nf1 and Nf2 that represent previously unappreciated candidates for genes involved in normal Nf1/Nf2 signaling, and/or Nf1/Nf2-mediated disease progression.

- The development of technology to derive quantitative phenotypic profiles of cells now facilitates the rapid screening for both genes and small-molecules that could modify the phenotype of Nf1 and Nf2 deficient cells.

Reportable Outcomes

<u>Manuscripts:</u>

Bakal, C., Aach, J., Church, G.M., and Perrimon, N. "Defining the Components of Local Signaling Networks that regulate Cell Morphology using stochastic labeling and Quantitative Morphological Signatures" (*Manuscript in preparation*)

<u>Presentations:</u>

"Making a RHOad map: modeling the local network of Rho signaling using phenotypic and transcriptional profiling" FASEB Summer Research Conference on Regulation and Function of Small GTPases. Saxtons River, VT, USA. July 2006.

"Building a "RHOad map". Modeling Rho Signaling Networks Through the Integration of High-Content Multidimensional Data Sets" Cold Spring Harbor/Wellcome Trust Conference on Interactome Networks. Hinxton, UK. August 2006.

Conclusions

Understanding the signaling pathways that regulate, and are regulated by, Nf1 and Nf2 are essential in the development of therapeutics to treat patients suffering from diseases that result from loss-of-function mutations in these diseases. In model systems, such as *Drosophila*, high-throughput genetic and chemical screens have been powerful tools to elucidate both components and inhibitors of a variety of signaling pathways. The execution and success of these screens is dependent of the development of experimental assays which serve as direct readouts of pathway activity. However, to date no such assay for use in high-throughput studies has been developed to monitor the activity of Nf1 or Nf2. **Thus prior to performing screens for genetic modifiers of *Nf1* or *Nf2* we aimed to develop an experimental readout of Nf1 and Nf2 signaling activity.**

In conclusion, we have developed a novel technology that can be used rigorously quantify and analyze single-cell morphology in an automated fashion. As a proof-of-concept we have analyzed morphological data derived from 249 different conditions, and defined phenoclusters of functionally related genes. We observe that *Nf1* and *Nf2* are members of distinct phenoclusters and that other genes in these clusters may be highly relevant to understanding role of *Nf1* and *Nf2* in promoting disease. **Furthermore, with the successful development of methods to determine quantitative phenotypic profiles of cells, performing screen for genetic or chemical, modifiers of *Nf1* or *Nf2* is now feasible.**

References

1.   J. A. Walker *et al.*, *Genes Dev* **20**, 3311 (Dec 1, 2006).
2.   D. H. Gutmann, *Hum Mol Genet* **10**, 747 (Apr, 2001).
3.   A. I. McClatchey, M. Giovannini, *Genes Dev* **19**, 2265 (Oct 1, 2005).
4.   G. H. Baeg, R. Zhou, N. Perrimon, *Genes Dev* **19**, 1861 (Aug 15, 2005).
5.   R. DasGupta, A. Kaykas, R. T. Moon, N. Perrimon, *Science* **308**, 826 (May 6, 2005).
6.   K. Nybakken, S. A. Vokes, T. Y. Lin, A. P. McMahon, N. Perrimon, *Nat Genet* **37**, 1323 (Dec, 2005).
7.   A. Friedman, N. Perrimon, *Nature* **444**, 230 (Nov 9, 2006).
8.   J. A. Williams, H. S. Su, A. Bernards, J. Field, A. Sehgal, *Science* **293**, 2251 (Sep 21, 2001).
9.   D. N. Chadee, J. M. Kyriakis, *Nat Cell Biol* **6**, 770 (Aug, 2004).
10.   D. H. Gutmann *et al.*, *Hum Mol Genet* **10**, 3009 (Dec 15, 2001).
11.   M. Boutros *et al.*, *Science* **303**, 832 (Feb 6, 2004).
12.   B. Dasgupta, D. H. Gutmann, *Curr Opin Genet Dev* **13**, 20 (Feb, 2003).
13.   F. Piano *et al.*, *Curr Biol* **12**, 1959 (Nov 19, 2002).
14.   K. C. Gunsalus *et al.*, *Nature* **436**, 861 (Aug 11, 2005).
15.   A. A. Kiger *et al.*, *J Biol* **2**, 27 (2003).
16.   H. Wang *et al.*, *Dev Cell* **10**, 117 (Jan, 2006).
17.   S. R. Singh *et al.*, *Dev Growth Differ* **48**, 169 (Apr, 2006).
18.   M. Bienz, *Curr Biol* **15**, R64 (Jan 26, 2005).
19.   V. Bennett, A. J. Baines, *Physiol Rev* **81**, 1353 (Jul, 2001).
20.   K. B. Hoover, P. J. Bryant, *Dev Genes Evol* **212**, 230 (Jun, 2002).
21.   P. Laprise *et al.*, *Dev Cell* **11**, 363 (Sep, 2006).

Appendicies

Table 1: Cell states used for classifier determination. Using Neural-Network based approaches we attempted to derive non-linear functions that could be used to classify each cell state (left-hand column) from the sixteen others in multi-dimensional space. These cell states were chosen for this analysis based on the fact they were qualitatively distinguishable.

Condition/Cell-type	Characteristic Phenotype by Visual Inspection
CG3799 full-length	Long, bipolar shaped cells.
CG3799 RNAi	Long, bipolar cells (very similar to overexpression of CG3799)
GFP	Polar cells with leading-edge lamellipodia, long filipodia, and marked trailing edge.
N-RhoGEF3	Very small, often perfectly round cells with little variation between cells.
N-Sif	Very large cells with extensive lamellipodia.
N-Sif + Sif full-length	-
Rac RNAi	Highly retracted cells with long, very thin filaments
RacF28L (Fast-cycling activated Rac)	Extensive lamellipodia and filipodia formation. Loss of polarity. Increase in cell size.
RacF28L + RacG12V	-
RacG12V (GTP-locked activated Rac)	Extensive lamellipodia formation. Loss of polarity. Increase in cells size.
Rho RNAi	Irregularly shaped, often large cells. Typically appeared flat (but with few lamellipodia)
RhoF28L (Fast-cycling activated Rho)	Small compacted cells with jagged, "fuzzy" edges.
RhoG14V (GTP-locked activated Rho)	Extensive, long and irregular protrusions. Cells body appears small and retracted.
RhoGEF3 RNAi	Small round cells. Few protrusions
RhoV14 + RhoF28L	-
Sif full-length	None, appeared similar to control cells
Sif RNAi	Small round cells, sometimes with long filamentous outgrowths

Figure 1. Inhibiting Nf1 or Nf2 by dsRNA-mediated gene silencing results in distinct effects on cellular morphology. *Drosophila* BG-2 cells were transfected with plasmids encoding GFP alone (A), in combination with *Nf1* dsRNA (B), or *Nf2* dsRNA (C). Control BG-2 cells typically form extensive polarized lamellipodial protrusions at the leading edge of cells (red arrows), and coordinated retraction at the trailing edge (green arrows). In cells where *Nf1* or *Nf2* has been silenced by dsRNA, cells are highly rounded, retracted, and unpolarized. However cells where *Nf1* is inhibited by dsRNA still have some filamentous protrusions (chevrons), whereas inhibition of *Nf2* results in a complete absence of any protrusive activity. All scale bars represent 10 μm.

Figure 2. Phenotypic Profiling workflow. (A) Cultured *Drosophila* BG-2 cells are transfected with plasmids encoding GFP and are incubated in the presence of dsRNA for 4 days. Alternatively GFP-transfected cells are co-transfected with plasmids encoding RFP-tagged proteins. In some experiments, cells were both co-transfected with GFP and RFP-tagged proteins and treated with dsRNA. GFP-labeled cells are acquired by standard fluorescence microscopy and the images are processed by CellSegmenter. Single cell segments are subsequently analyzed whereupon ~150 different features regarding cell morphology and GFP-signal intensity are derived. (B) Typical features that make up phenotypic profiles.

Figure 3. The Identification of Local Networks that Regulate Distinct Aspects of Morphology. (A) Hierarchical clustering of the genes in the dataset (y-axis) by how cells score on the ΔN-Sif, ΔN-RhoGEF3, CG3799, RacF28L, RacV12, RhoF30L, and RhoV14 classifiers (x-axis). We define phenoclusters of genes as cluster with PCC > 0.80 which results in 41 total clusters comprising 17 multi-gene clusters and 24 singletons. All multi-gene clusters are identified in brackets on the right-hand side of the clustergram. Particular cell-types and their position in the clustergram are shown on the left-hand side. Based on their gene membership a number of clusters are determined to have unique roles in cell-morphology. (B) A phenocluster of genes of which *Nf1* is a prominent member (C) A phenocluster of genes of which *Nf2/merlin* is a prominent member. All scale bars represent 10 μm.
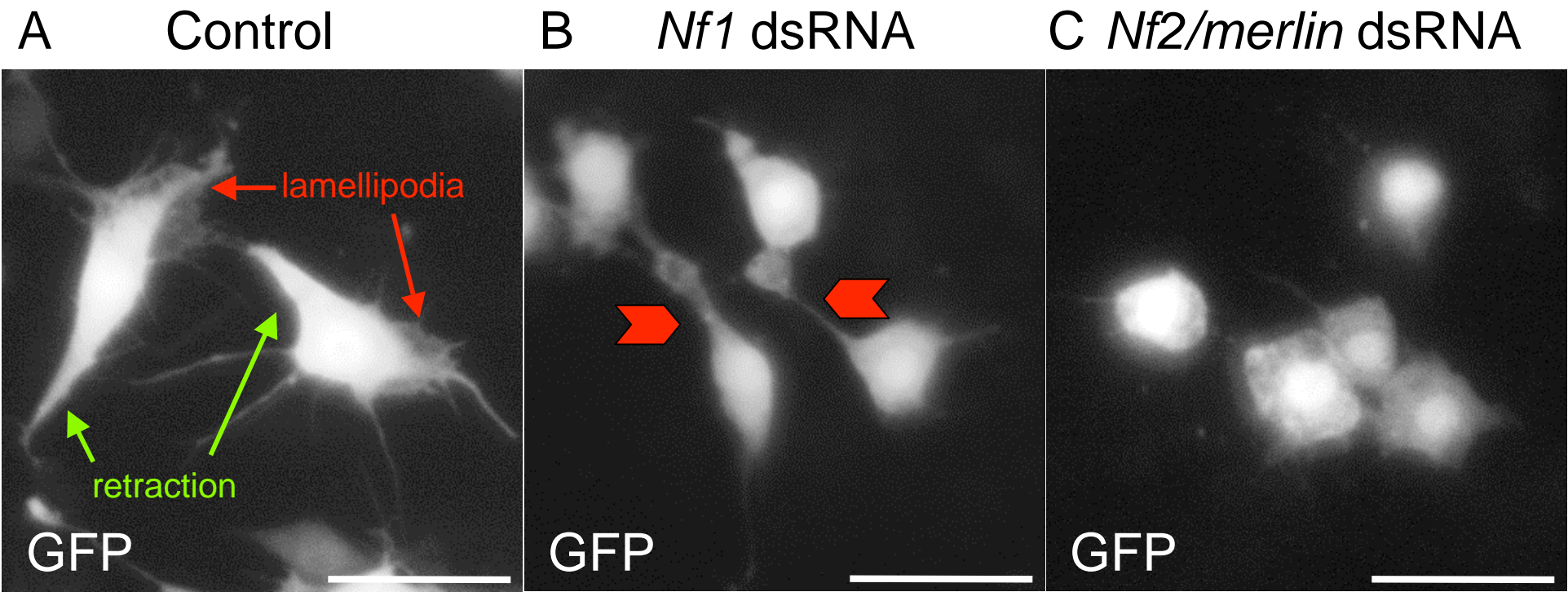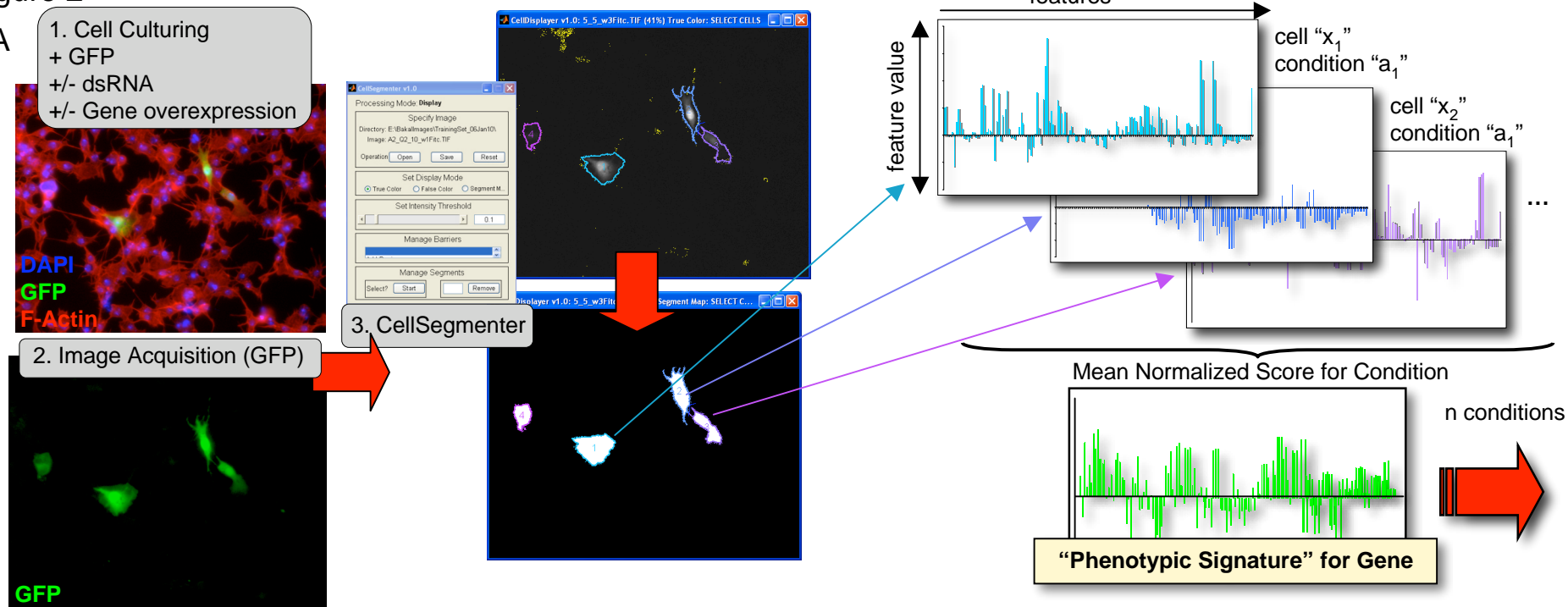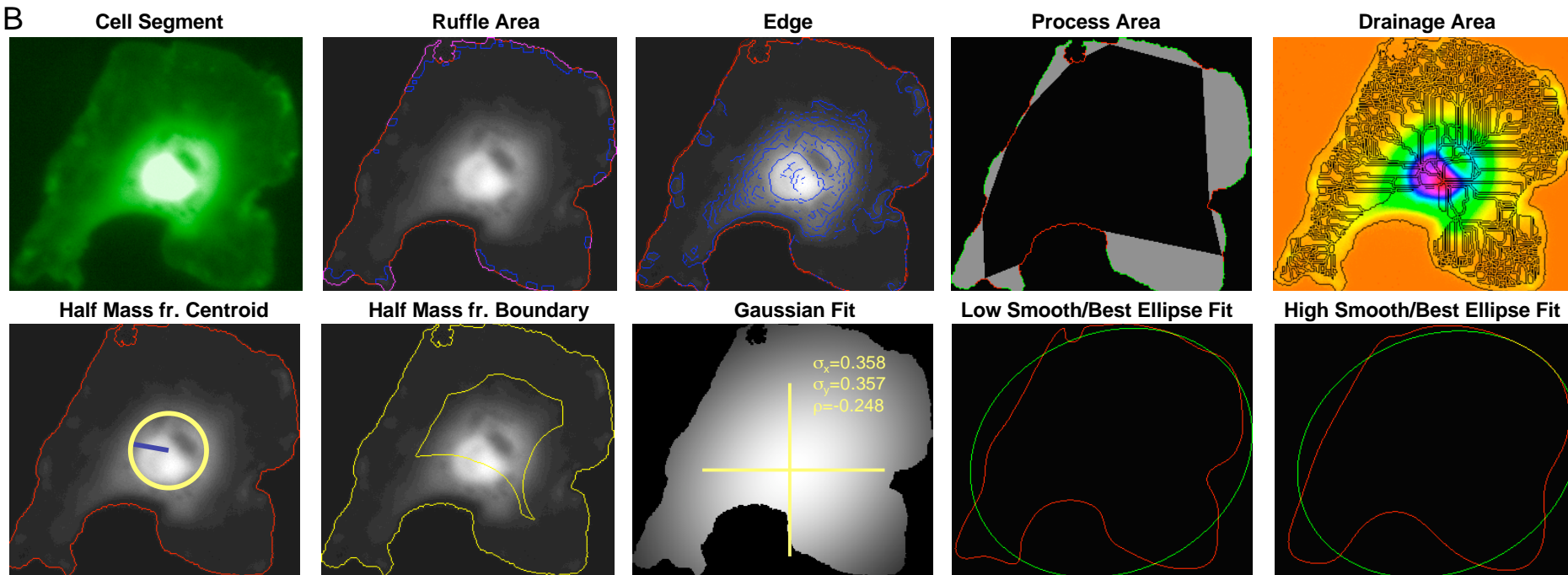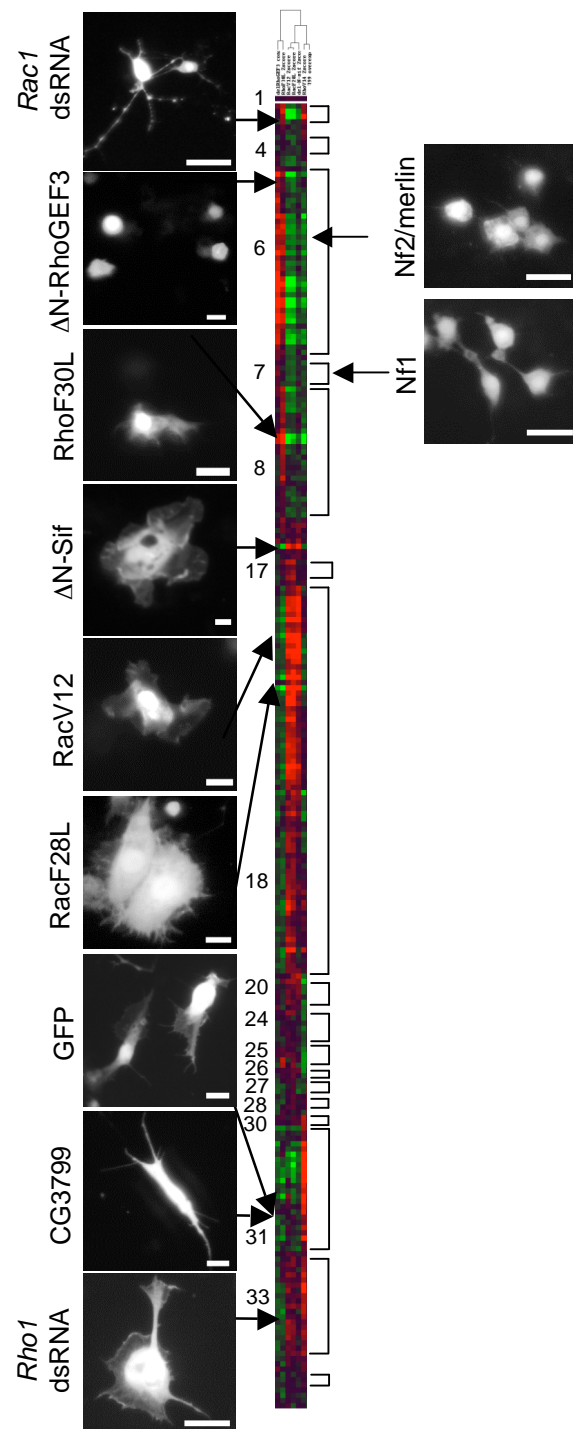
Figure 1

A   Control   B   *Nf1* dsRNA   C *Nf2/merlin* dsRNA

Figure 2

A

1. Cell Culturing
+ GFP
+/- dsRNA
+/- Gene overexpression

DAPI
GFP
F-Actin

2. Image Acquisition (GFP)

GFP

3. CellSegmenter

CellSegmenter v1.0

Processing Mode: **Display**

Specify Image
Directory: E:\BakalImages\TrainingSet_06Jan10\
Image: A2_G2_10_w1Fitc.TIF

Operation Open   Save   Reset

Set Display Mode
○ True Color ○ False Color ○ Segment M...

Set Intensity Threshold
[_____] 0.1

Manage Barriers

Manage Segments
Select? Start [____] Remove

CellDisplayer v1.0: 5_5_w3Fitc.TIF (41%) True Color: SELECT CELLS

Displayer v1.0: 5_5_w3Fit... Segment Map: SELECT C...

features

feature value

cell "x_1"
condition "a_1"

cell "x_2"
condition "a_1"

...

Mean Normalized Score for Condition

n conditions

"Phenotypic Signature" for Gene

B

| Cell Segment | Ruffle Area | Edge | Process Area | Drainage Area |

| Half Mass fr. Centroid | Half Mass fr. Boundary | Gaussian Fit | Low Smooth/Best Ellipse Fit | High Smooth/Best Ellipse Fit |

$\sigma_x = 0.358$
$\sigma_y = 0.357$
$\rho = -0.248$

Figure 3